Hexokinase 2 expression in apical enterocytes correlates with inflammation severity in patients with inflammatory bowel disease

Saskia Weber-Stiehl[1*], Jan Taubenheim[2*], Lea Järke[1*], Christoph Röcken[3], Stefan Schreiber[4], Konrad Aden[1,4], Christoph Kaleta[2], Philip Rosenstiel[1], Felix Sommer[1]

[1] Institute of Clinical Molecular Biology, University of Kiel, Rosalind-Franklin-Straße 12, 24105 Kiel, Germany

[2] Institute of Experimental Medicine, University of Kiel, Michaelisstr. 5, 24105 Kiel, Germany

[3] Department of Pathology, University Hospital Schleswig-Holstein, Campus Kiel, Arnold-Heller-Straße 3/House U33, 24105 Kiel, Germany

[4] Department of Internal Medicine I, University Hospital Schleswig-Holstein, Campus Kiel, 24105 Kiel, Germany

[*] These authors contributed equally with shared first authorship.

Correspondence: Felix Sommer, Institute of Clinical Molecular Biology (IKMB), Christian-Albrechts-University (CAU) Kiel, Rosalind-Franklin-Str. 12, Kiel D-24105, Germany; tel: +49(0) 431/500-15146; email: f.sommer@ikmb.uni-kiel.de

Keywords: inflammation / hexokinase / HK2 / human biopsies

Abstract

Background: Inflammation is characterized by a metabolic switch promoting glycolysis and lactate production. Hexokinases (HK) catalyze the first reaction of glycolysis and inhibition of epithelial HK2 protected from colitis in mice. HK2 expression has been described as elevated in patients with intestinal inflammation, however there is conflicting data from few cohorts especially with severely inflamed individuals, thus systematic studies linking disease activity with HK2 levels are needed.

Methods: We examined the relationship between HK2 expression and inflammation severity using bulk transcriptome data derived from the mucosa of thoroughly phenotyped patients suffering from intestinal inflammation of two independent cohorts. Analyzing publicly available single cell RNA sequencing data and performing immunofluorescence on colonic biopsies of unrelated patients with intestinal inflammation confirmed the RNA-based findings on cellular and protein level.

Results: HK2 expression gradually increased from mild to intermediate inflammation, yet strongly declined at high inflammation scores. Expression of epithelial marker genes also declined at high inflammation scores, whereas that of candidate immune marker genes increased, indicating a cellular remodeling of the mucosa during inflammation with an infiltration of HK2-negative immune cells and a loss of the apical epithelium – the main site of HK2 expression. Normalizing for the enterocyte loss clearly identified epithelial HK2 expression as gradually increasing with disease activity and remaining elevated at high inflammation scores. HK2 protein expression was mostly restricted to brush border enterocytes and these cells along with HK2 levels vanished with increasing disease severity.

Conclusions: Our findings clearly define dysregulated epithelial HK2 expression as an indicator of disease activity in intestinal inflammation and suggest targeted HK2-inhibition as a potential therapeutic avenue.

Background

Prevalence of inflammatory bowel disease (IBD) is rising globally causing severe health issues and drastically reducing quality of life. These diseases are multifactorial with complex interactions of multiple genetic and environmental factors[1]. Despite decades of intense research, the exact etiology of IBD remains mostly unknown limiting treatment options[2]. In recent years it became evident that ongoing inflammation is characterized by changes in metabolic activity, in particular glucose metabolism[3–5]. Hexokinases (HK) catalyze the first and irreversible step of glycolysis – the phosphorylation of glucose to glucose-6-phosphate – and are therefore crucial for glucose metabolism and maintenance of homeostatic body functions. In mammals, five HK isoenzymes have been identified: HK1, HK2, HK3, GCK (Glucokinase) and HKDC1 (HK domain containing 1). Each of these HK isoenzymes display specific tissue expression patterns and glucose affinities. HK2 is of particular interest as it is the most abundant HK member within the intestine, exerts high HK activity, responds to various internal as well as external stimuli and shows elevated levels during inflammation[6]. Recently, we further revealed an upregulated expression of HK2 specifically in inflamed compared to non-inflamed tissue of the same patient, irrespective of the type of intestinal inflammation and demonstrated that ablation of HK2 in intestinal epithelial cells (IEC) protects from acute intestinal inflammation, suppresses cell death and alters mitochondrial function[6]. These findings placed HK2 as a molecular target to treat intestinal inflammation. However, when expanding our research about the role of HK2 in intestinal inflammation, we encountered transcriptome datasets with contradictory findings of either an unaltered HK2 expression or even downregulation, especially in severely inflamed patients undergoing bowel resection[7]. We therefore aimed to investigate the cause of this apparent contradiction with the goal to clarify the relation between HK2 expression and intestinal inflammation. Here, we show that with increasing inflammation severity the intestinal mucosa is gradually remodeled, which comprises a partial loss of the apical epithelium – the primary source of HK2 expression – and a simultaneous infiltration of immune cells. Normalizing for this cellular remodeling clearly demonstrates a gradual upregulation of HK2 expression with severity of intestinal inflammation.

Methods

Human studies

We used mucosal transcriptomic data and fixed intestinal specimen of two independent large longitudinal clinical studies, namely the EMED[9] (191 samples) and FUTURE[8] (87 samples) cohorts (trial IDs: EudraCT number 2016-000205-36 and ClinicalTrials.gov NCT02694588), for which accompanying disease activity scores (Harvey-Bradshaw Index (HBI)/Mayo Score) were available (see Table S1 for cohort clinical characteristics). Note that multiple samples were collected from each patient. Sample origin was incorporated in all following analyses. The HBI[26] is used to quantify disease activity in patients suffering from Crohn's disease (CD), one of the two IBD subtypes. Here, variables such as general well-being, abdominal pain and abdominal mass with each having scores of 0-3, as well as the number of liquid stools per day (1 point per stool) and other complications (1 point per complication) yield the "open-ended" total score (Table S3). The Mayo score is used for ulcerative colitis (UC), the other clinical IBD subtype. This scoring system accounts for general well-being, rectal bleeding, endoscopic results and stool frequency with scores of 0-3 per category for an overall score ranging from 0 to 12 (Table S3). To facilitate a direct comparison of both scores despite them being "open-ended" and "discrete", we calculated a general inflammation score by setting the highest score in the dataset for each HBI and Mayo score to 1 and scaled the score of each patient accordingly (see Table S3).

Transcriptome data analysis

RNA sequencing data derived from mucosal biopsies of patients with various grades of intestinal inflammation were retrieved from two previously published IBD cohorts[8,9]. Read counts were transformed to Transcripts Per Million (TPM) values to normalize for differential sequencing depths among samples. TPM data were then plotted per sample against the inflammation score using R (version 4.2.2) and ggplot2 (3.4.3). Trendlines were calculated including all data points and using the distance to the actual location as a weight to enable a robust calculation and avoiding overfitting especially in areas of scarce sampling. To test for an association of gene expression to changes in the inflammation score we used variance-stabilization transformation of raw read counts and fitted linear mixed models with following form: vst(geneExpression) ~ Age + Sex + Diagnosis + InflammationScore. Statistical analyses

106 were performed using R (version 4.2.2[27] with the following packages: lm4 (version 1.1-29)[28],
107 lmerTest (version 3.1-3)[29], car (version 3.0-13)[30], ggplot2 (version 3.3.6)[31] and DESeq2
108 (version 1.38.3)[32].
109
110 **Cellular deconvolution**
111 We deconvoluted the bulk RNA data using the MuSiC package (version 1.0.0)[10] with default
112 values. As reference, we used a single cell data set from UC patients described in a study by
113 Smillie et. al.[11]. The original single cell data set was split in "epithelial", "immunogenic" and
114 "stromal" subsets, which we rejoined in our analysis. Due to limited resolution in
115 deconvolution approaches and to reduce cell diversity, we pooled ontogenetically closely
116 related cell types (Table S4). We restricted the analysis to the eight most abundant cell types.
117
118 **Single cell RNA sequencing**
119 Single cell data was obtained from the Single Cell Portal (accession SCP259) initially described
120 by Smillie and colleagues[11]. The different cell populations were rejoined and general quality
121 controls were performed. In short, we filtered cells with read counts below 1000 (low quality).
122 Further, we removed cells with less than 200 or with more than 2720 (two-fold of the
123 standard deviation of expressed genes across all cells) differently expressed genes to account
124 for spurious sequencing depth and removal of duplicates. All cells with a mitochondrial RNA
125 content above 5% were also removed. For plotting, gene expression values where log-
126 transformed. Plotting and quality filtering was performed in R (version 4.2.2) using ggplot2
127 (version 3.4.3) and Seurat (version 4.4.0)[33].
128
129 **Immunofluorescence**
130 5 µm sections of paraffin-embedded colonic biopsies were deparaffinized with Xylol
131 substitute (Roth), incubated in citrate buffer for 3 minutes and subsequently blocked in 5 %
132 BSA-PBS and 0,2 % TritonX for 30 minutes. Primary anti-E-cadherin (1:400 in 1 % BSA, #3195,
133 Cell Signaling Technology) and anti-Hexokinase 2 (1:500 in 1% BSA, Cat# NBP2-02272, Novus
134 Biologicals, Colorado, US) antibodies were incubated over-night. Sections were washed,
135 incubated with secondary antibodies (Alexa Fluor 488 goat anti mouse, Invitrogen, A32731
136 and Alexa Fluor 555 goat anti rabbit, Invitrogen, A21430) for 45 minutes at room
137 temperature. DAPI (1:40000 in PBS, D9542, Sigma Aldrich, St. Louis, US) was used for DNA

counterstaining. Slides were mounted using antifade mounting media (DAKO, Hovedstaden, Denmark). The quantitative analysis was performed using fluorescence microscopy for stained samples using the imager Z1 microscope (ZEISS, Jena, Germany) and ZEN software (version 3.0). Images were taken by a digital camera system (AxioCam HrC/HrM, Zeiss, Jena, Germany) and ApoTome (ZEISS, Jena, Germany). Fluorescence signal intensity was measured using Fiji/ImageJ software.

Statistics

General statistical analyses were performed using the GraphPad Prism 9 (GraphPad Software Inc., La Jolla, USA). For pairwise comparisons the Mann-Whitney-U test was used whereas for multiple comparisons one-way ANOVA with false discovery rate (FDR) correction were performed. Data are shown as mean ± standard error of the mean (SEM). A p-value of ≤ 0.05 was considered as significant (*). A p-value of ≤ 0.01 was considered as strongly significant (**) and p-value of ≤ 0.001 as highly significant (***). For longitudinal data, linear mixed effect models were fitted where gene expression was used as dependent variable, while inflammation score and patient ID were fixed and random factors. The models were fitted using lme4 (version 1.1-31) and statistical testing for coefficients was performed using lmerTest (version 3.1-3). Model validity was tested against a null-model using log-likelihood ratio tests and model assumption were evaluated by diagnostic plotting of model residuals, data point influence strength and random factor fitting.

158 **Results**

159 **Epithelial HK2 expression increases with high inflammation scores**

160 To determine a possible correlation of HK2 expression and disease activity, we analyzed RNA
161 sequencing (RNA-seq) data derived from intestinal biopsies of patients suffering from IBD of
162 two independent clinical studies[8,9], for which accompanying disease activity scores for each
163 sample were available (Table S1). This analysis revealed that HK2 expression initially increased
164 gradually reaching peak expression at mid disease activity (inflammation score ~ 0.4) and then
165 declined with high inflammation scores (Figure 1A). As within the intestine HK2 is mainly
166 expressed by epithelial cells of the apical mucosa (Figure S1), we hypothesized that with very
167 high levels of inflammation these apical epithelial cells and therefore also the main site of HK2
168 expression might be lost due to shedding and apoptosis or transdifferentiation resulting in
169 decreased HK2 expression levels in bulk RNA-seq data. To investigate this hypothesis, we
170 assessed the expression levels of three different epithelial marker genes, namely E-cadherin
171 (*ECAD*), epithelial cell adhesion molecule (*EPCAM*) and Villin1 (*VIL1*). Supporting our
172 hypothesis, the expression levels of these epithelial markers were all declining with increasing
173 inflammation severity (Figure 1B-D), which indicates progressive epithelial damage caused by
174 the inflammation. To account for this epithelial loss, we then normalized the expression of
175 HK2 to that of these epithelial markers, thereby yielding an epithelial HK2 expression.
176 Importantly, epithelial HK2 expression gradually increased in correlation to disease activity
177 and then remained elevated at high inflammation scores (Figure 1E). To test whether the
178 observed expression changes were unique to the combined clinical cohorts, we also
179 performed these analyses separately for each clinical cohort (Figure S2). Importantly, we
180 observed for both clinical cohorts the same changes in *HK2*, *ECAD*, *EPCAM*, *ECAD* and
181 epithelial HK2 expression. We also tested for potential differences between the two main
182 types of IBD, Crohn´s disease (CD) and ulcerative colitis (UC) and found similar responses both
183 for CD and UC (Figure S3). Finally, correlation of HK2 expression with disease severity was
184 confirmed using linear regression models (Figure S4 and Table S2).

185

186 **Immune cell infiltration during intestinal inflammation**

187 Another source for cellular remodeling during inflammation is tissue infiltration by immune
188 cells. Using the bulk RNA-seq data we also investigated the proportions of various immune
189 cell types in relation to disease severity. First, we performed a candidate gene-based analysis
190 and chose several immune marker genes to assess infiltration of T cells, T helper 1 (Th1) cells,
191 T helper 2 (Th2) cells, B cells, basophils, neutrophils, eosinophils, and macrophages (Figure
192 2A). In contrast to *HK2* and the epithelial marker genes, the expression of these individual
193 immune cell genes increased with the inflammation score. However, slight alterations in the
194 expression patterns could be observed, mostly depending on the immune cell type.
195 Expression of the T cell marker genes *TRAC*, *CD3D* and *CD3E,* the B cell marker gene *CD19,* the
196 eosinophil marker gene *CCR2*, the neutrophil marker genes *CD14* and *CXCR4* as well as the
197 basophil marker genes *ITGA2B* and *ITGA4* all gradually increased in a linear fashion with the
198 inflammation score (Figure 2). In contrast, the marker genes for Th2 (*IL4*, *IL5*, *IL13*), Th1 (*IFNG*,
199 *IL12*) cells and macrophages (*ITGAM*, *IL1B*) all only displayed biphasic expression patterns
200 with a first phase characterized by slight increases in expression until an inflammation score
201 of approximately 0.5 and a second phase at higher disease severity characterized by larger
202 changes in their expression. The greatest expression changes were detected for the
203 macrophage marker genes *ITGAM* and *IL1B* suggesting the greatest relative increase of these
204 cells with increasing disease activity. Normalizing *HK2* expression to the candidate immune
205 cell genes revealed gradual declines with increasing inflammation scores for all tested
206 immune cell types indicating that the immune cell infiltration leads to more cells present in
207 the mucosa, which do not or only express very little *HK2* (Figure 2B).

208 Next, we moved from the candidate gene-based to a systematic cellular deconvolution of the
209 bulk RNA-seq data using MuSiC[10]. This program uses a reference single cell data set and cell
210 type-specific expression profiles to derive the abundance of the individual cell types from bulk
211 RNA-seq data. We restricted this analysis to the eight most abundant cell types. The
212 proportion of epithelial cells gradually declined with increasing inflammation scores whereas
213 the proportion of macrophages, B cells and regulatory T cells increased (Figure 3A). The
214 proportion of mast, cytotoxic T cells and dendritic cells remained mostly unchanged.
215 Therefore, this data indicates a massive gradual cellular remodeling of the intestinal mucosa
216 during inflammation and the findings of the systematic cellular deconvolution supported
217 those of the candidate gene-based analyses. Furthermore, the drastic decrease in the

218 proportion of epithelial cells with increasing inflammation scores demonstrates again that the
219 main source of *HK2* expression is lost during the disease course. This is therefore also
220 reflected by the outcome that after accounting for the abundance of epithelial cells the
221 normalized epithelial *HK2* expression gradually increased with disease severity (Figure 3B).

222

223 **Apical HK2 expression in mature enterocytes correlates with inflammation severity**

224 To validate the transcriptome data and to elucidate the biogeography of the changes in tissue
225 architecture in relation to HK2 expression, we performed immunostainings on colonic
226 biopsies of an independent set of UC patients that had been thoroughly scored for histological
227 disease severity (Nancy score). HK2 protein levels increased non-significantly in mildly
228 inflamed (score 1) compared to non-inflamed specimen (score 0) and remained unaltered at
229 medium or strong inflammation (scores 2 and 4) (Figure 4A,C). In contrast, protein levels of
230 the epithelial marker E-cadherin (ECAD) were unchanged in mild (score 1) but non-
231 significantly reduced at medium or strong inflammation (scores 2 and 4) compared to non-
232 inflamed control samples (Figure 4A,C). Notably, structural epithelial damage of inflamed
233 biopsies was detectable with increasing inflammatory scores (Figure 4C) with loss of epithelial
234 cells and an infiltration of other cells, probably immune cells, into the inflamed mucosa. In
235 addition, many epithelial cells that were not shed but still present at the inflamed site had
236 reduced ECAD expression, which could indicate transdifferention of these inflamed apical
237 enterocytes. Normalizing the HK2 protein levels to those of ECAD revealed that epithelial HK2
238 protein levels (Figure 4B) significantly increased with inflammation regardless of disease
239 severity (scores 1-4). This epithelial HK2 protein expression in inflamed intestinal mucosal
240 biopsies mirrored and confirmed the transcript patterns of the RNA sequencing analysis.

241 Furthermore, we used recently-published data from single cell RNA sequencing of mucosal
242 biopsies from IBD patients[11] to investigate the *HK2* expression on a cellular level in relation to
243 intestinal inflammation. This analysis of single cell RNA sequencing data confirmed our
244 findings from the bulk RNA sequencing and immunofluorescence, as *HK2* was mainly
245 expressed by mature enterocytes and then followed by goblet cells and immature
246 enterocytes (Figure 5A,B). Next, we checked for *HK2* expression pattern in enterocytes at
247 different inflammatory stages (healthy vs. inflamed vs. non-inflamed) and found that the
248 lowest *HK2* expression can be observed in healthy controls, while cells from inflamed samples

249 showed an increased HK2 expression (Figure 5C). Non-inflamed samples had intermediate
250 *HK2* expression levels (Figure 5C), which indicates that HK2 expression is dysregulated in
251 enterocytes of IBD patients also in the absence of an overt inflammation. This pattern of *HK2*
252 expression was also present although less predominant in immature enterocytes and goblet
253 cells. Finally, we looked into the number of these three cell types that are detected in the
254 three health states and found that mature and immature enterocytes are lost during
255 inflammation, while incomplete recovery can be observed in non-inflamed tissue of IBD
256 patients (Figure 5D). Altogether, the single cell data therefore supports a cellular
257 reprogramming during inflammation with loss of mature enterocytes (the main cell type of
258 the apical epithelium) and a dysregulated *HK2* expression in inflamed apical epithelial cells.

259 In summary, both the RNA and protein data clearly demonstrate that epithelial HK2 was
260 overexpressed during intestinal inflammation, which highlights HK2 as an indicator of active
261 disease. Building upon previous findings from murine models that inhibition of HK2
262 expression either genetically or via the microbial metabolite butyrate protect from
263 experimental colitis[6], these new data now show that indeed HK2 expression is dysregulated
264 in the mucosa of patients with active inflammation and therefore suggest that targeting HK2
265 may represent a promising approach to suppress intestinal inflammation in humans.

266 **Discussion**

267 There is a growing need for valid disease biomarkers and molecular targets for intestinal
268 inflammation as prevalence is increasing and despite significant efforts the cause of these
269 diseases remains unknown. In a recent study, HK2 was identified as upregulated under
270 inflammatory conditions in mice and humans irrespective of disease subtype (CD, UC or non-
271 IBD colitis) and suppressing HK2 expression even protected from experimental colitis[6] placing
272 HK2 as a potential disease marker. However, we found other transcriptome datasets
273 generated from severely inflamed patients in which HK2 expression was unaltered or even
274 reduced[7]. Here, we therefore thoroughly investigated the relationship between HK2
275 expression and disease severity by analyzing transcriptome data derived from intestinal
276 biopsies of patients with intestinal inflammation for which corresponding data on disease
277 severity (HBI, Mayo score, Nancy score) were available. In addition, we performed cellular
278 deconvolution analyses of the RNA sequencing data to infer the changes in cell proportions
279 during inflammation. Finally, we used immunofluorescence staining to clarify the changes in
280 HK2 protein biogeography in the mucosa during inflammation. Using these approaches, we
281 demonstrated that raw HK2 RNA and protein expression at first gradually increased with the
282 inflammation scores, yet after reaching a critical inflammation score HK2 expression declined
283 again at very severe inflammation. These findings integrate the seemingly conflicting data
284 from previous studies[7,12–14] by linking HK2 expression to disease severity. We further were
285 able to demonstrate that loss of HK2 expression at high inflammation levels was dependent
286 on the disruption of brush border enterocytes as both the expression of epithelial marker
287 genes were decreasing with the inflammation score and immunofluorescence analyses clearly
288 pointed to a destruction of the apical epithelium – the main site of HK2 expression[15,16]. These
289 findings are in line with clinical practice, in which epithelial damage is a key criterion to classify
290 an increasing inflammatory state during IBD[17], for example with epithelial erosion being a
291 feature of histological inflammation in the Nancy score. By analyzing single cell RNA
292 sequencing data derived from an independent set of UC patients, we confirmed that in the
293 gut epithelial cells are the main source of *HK2* expression, both in terms of per cell expression
294 as well as the number of cells contributing to overall expression (Figure 5). These cells are
295 consequently lost due to increasing inflammation in the single cell data set, which would
296 explain the decrease of *HK2* expression at high levels of inflammation[11]. Finally, we were able

297 to deconstruct the simultaneous epithelial erosion and immune cell infiltration into the
298 submucosa during intestinal inflammation from the RNA sequencing data. Based on the
299 overall abundance and their induction (fold change) during inflammation, infiltrating
300 macrophages seemed most relevant, but also other cell types such as B cells increased in
301 proportion. Especially the expansion of macrophages could be important and contributing to
302 the loss of epithelial cells and therefore HK2 expression during inflammation as IL-1β
303 interferes with the tight junction complexes between IECs[11–13] and thereby increases
304 intestinal permeability[21]. Similar to epithelial erosion, immune cell infiltration is a classical
305 feature of inflammation and used in clinical practice to histologically evaluate disease
306 severity, in particular as a feature of the Nancy score[22]. In addition, transdifferentiation of
307 HK2-positive mature enterocytes into other cell types such as HK2-negative immature
308 enterocytes and stem cells[23,24] or maybe even into mesenchymal cells as during epithelial–
309 mesenchymal transition [25] could also contribute to a reduction of HK2 levels in the inflamed
310 mucosa. In summary, our findings imply that during the course of inflammation, changes in
311 the cellular composition of the mucosa, i.e. loss of brush border epithelial cells expressing
312 high levels of HK2 and a corresponding massive recruitment of immune cells expressing little
313 to no HK2 to the site of inflammation, affect the overall bulk HK2 expression leading to an
314 overall reduction despite higher expression levels in fewer and fewer HK2-positive cells
315 (Figure 6). Overall, we want to highlight the importance of taking into consideration the
316 biogeography and changes in cell type expression ratios, when trying to identify disease
317 biomarkers, especially regarding complex diseases such as intestinal inflammation involving
318 various internal and external factors. Most previous studies used bulk expression data in the
319 search for disease biomarkers or therapeutic targets and therefore may have missed other
320 locally restricted but disease relevant genes like *HK2*. In our analyses HK2 expression was only
321 significantly associated with disease severity after considering epithelial cell abundance
322 (Figure 1E and Figure 3B) and we speculate that this pattern will also hold true for other genes
323 with an apical or otherwise restricted expression. For example, other hexokinases (HK1,
324 HKDC1), proteins responsible for the uptake of dietary nutrients (e.g. SGLT1, SLC15A1) or
325 those contributing to the intestinal epithelial barrier (e.g. CLDN15, ZO-1) also show a
326 predominant or even restricted apical expression and therefore possibly have not yet been
327 identified as disease biomarker during severe intestinal inflammation due to the loss of their
328 primary expression site. Notably, epithelial remodeling not only includes the partial loss of

329 apical enterocytes and infiltration of lymphocytes, but also includes hyperregeneration,
330 metaplasia and a loss of goblet cells. The advent of single cell technologies such as single cell
331 RNA sequencing promise to pave the way for more refined analyses that will enable the
332 discovery of more suitable disease markers and to enhance our understanding of the
333 molecular and cellular mechanisms during disease progression.

334 **Conclusions**

335 HK2 has not yet been described as IBD risk gene, most probably due to its site-restricted
336 expression, but here we were able to show an association of HK2 and epithelial status during
337 intestinal inflammation. Therefore, epithelial HK2 expression correlates with disease severity
338 making it a useful indicator of intestinal inflammation and highlighting the therapeutic
339 potential of targeting HK2. However ultimately, clinical studies are required to indeed
340 demonstrate the feasibility and efficacy of a HK2-targeted intervention in IBD patients.

341 **References**

342 1. Kaplan, G. G. & Windsor, J. W. The four epidemiological stages in the global evolution of
343 inflammatory bowel disease. *Nat Rev Gastroenterol Hepatol* **18**, 56–66 (2021).
344 2. Kaplan, G. G. The global burden of IBD: from 2015 to 2025. *Nat Rev Gastroenterol*
345 *Hepatol* **12**, 720–727 (2015).
346 3. Rath, E. & Haller, D. Intestinal epithelial cell metabolism at the interface of microbial
347 dysbiosis and tissue injury. *Mucosal Immunology* **15**, 595–604 (2022).
348 4. Gaber, T., Strehl, C. & Buttgereit, F. Metabolic regulation of inflammation. *Nature*
349 *Reviews Rheumatology* **13**, 267–279 (2017).
350 5. Soto-Heredero, G., Gómez de las Heras, M. M., Gabandé-Rodríguez, E., Oller, J. &
351 Mittelbrunn, M. Glycolysis – a key player in the inflammatory response. *FEBS J* **287**,
352 3350–3369 (2020).
353 6. Hinrichsen, F. *et al.* Microbial regulation of hexokinase 2 links mitochondrial metabolism
354 and cell death in colitis. *Cell Metab* **33**, 2355-2366.e8 (2021).
355 7. Peters, L. A. *et al.* A functional genomics predictive network model identifies regulators of
356 inflammatory bowel disease. *Nat Genet* **49**, 1437–1449 (2017).
357 8. Schreiber, S. *et al.* Therapeutic Interleukin-6 Trans-signaling Inhibition by Olamkicept
358 (sgp130Fc) in Patients With Active Inflammatory Bowel Disease. *Gastroenterology* **160**,
359 2354-2366.e11 (2021).
360 9. Zeissig, S. *et al.* Vedolizumab is associated with changes in innate rather than adaptive
361 immunity in patients with inflammatory bowel disease. *Gut* **68**, 25–39 (2019).
362 10. Wang, X., Park, J., Susztak, K., Zhang, N. R. & Li, M. Bulk tissue cell type deconvolution
363 with multi-subject single-cell expression reference. *Nat Commun* **10**, 380 (2019).

364 11. Smillie, C. S. *et al.* Intra- and Inter-cellular Rewiring of the Human Colon during
365 Ulcerative Colitis. *Cell* **178**, 714-730.e22 (2019).
366 12. Marigorta, U. M. *et al.* Transcriptional risk scores link GWAS to eQTLs and predict
367 complications in Crohn's disease. *Nat Genet* **49**, 1517–1521 (2017).
368 13. Haberman, Y. *et al.* Pediatric Crohn disease patients exhibit specific ileal transcriptome
369 and microbiome signature. *J. Clin. Invest.* **124**, 3617–3633 (2014).
370 14. Quraishi, M. N. *et al.* A Pilot Integrative Analysis of Colonic Gene Expression, Gut
371 Microbiota, and Immune Infiltration in Primary Sclerosing Cholangitis-Inflammatory
372 Bowel Disease: Association of Disease With Bile Acid Pathways. *Journal of Crohn's and*
373 *Colitis* **14**, 935–947 (2020).
374 15. Sommer, F., Nookaew, I., Sommer, N., Fogelstrand, P. & Bäckhed, F. Site-specific
375 programming of the host epithelial transcriptome by the gut microbiota. *Genome Biol*
376 **16**, 62 (2015).
377 16. The Tabula Muris Consortium *et al.* Single-cell transcriptomics of 20 mouse organs
378 creates a Tabula Muris. *Nature* **562**, 367–372 (2018).
379 17. Guan, Q. A Comprehensive Review and Update on the Pathogenesis of Inflammatory
380 Bowel Disease. *Journal of Immunology Research* **2019**, 1–16 (2019).
381 18. Coccia, M. *et al.* IL-1β mediates chronic intestinal inflammation by promoting the
382 accumulation of IL-17A secreting innate lymphoid cells and CD4+ Th17 cells. *Journal of*
383 *Experimental Medicine* **209**, 1595–1609 (2012).
384 19. Chotikatum, S., Naim, H. Y. & El-Najjar, N. Inflammation induced ER stress affects
385 absorptive intestinal epithelial cells function and integrity. *International*
386 *Immunopharmacology* **55**, 336–344 (2018).

387 20. Lin, Y. *et al.* Non-hematopoietic STAT6 induces epithelial tight junction dysfunction and
388 promotes intestinal inflammation and tumorigenesis. *Mucosal Immunology* **12**, 1304–
389 1315 (2019).
390 21. He, L. *et al.* Gut Epithelial Vitamin D Receptor Regulates Microbiota-Dependent Mucosal
391 Inflammation by Suppressing Intestinal Epithelial Cell Apoptosis. *Endocrinology* **159**,
392 967–979 (2018).
393 22. Marchal-Bressenot, A. *et al.* Development and validation of the Nancy histological index
394 for UC. *Gut* **66**, 43–49 (2017).
395 23. Moor, A. E. *et al.* Spatial Reconstruction of Single Enterocytes Uncovers Broad Zonation
396 along the Intestinal Villus Axis. *Cell* **175**, 1156-1167.e15 (2018).
397 24. Wei, X. *et al.* Extensive jejunal injury is repaired by migration and transdifferentiation of
398 ileal enterocytes in zebrafish. *Cell Reports* **42**, 112660 (2023).
399 25. López-Novoa, J. M. & Nieto, M. A. Inflammation and EMT: an alliance towards organ
400 fibrosis and cancer progression. *EMBO Mol Med* **1**, 303–314 (2009).
401 26. Harvey, R. F. & Bradshaw, J. M. A Simple Index Of Crohn's-Disease Activity. *The Lancet*
402 **315**, 514 (1980).
403 27. R Core Team. *R: A Language and Environment for Statistical Computing*. (R Foundation
404 for Statistical Computing, Vienna, 2022).
405 28. Bates, D., Mächler, M., Bolker, B. & Walker, S. Fitting Linear Mixed-Effects Models Using
406 lme4. *Journal of Statistical Software* **67**, 1–48 (2015).
407 29. Kuznetsova, A., Brockhoff, P. B. & Christensen, R. H. B. lmerTest Package: Tests in Linear
408 Mixed Effects Models. *Journal of Statistical Software* **82**, 1–26 (2017).
409 30. Fox, J. & Weisberg, S. *An R Companion to Applied Regression*. (Sage, Thousand Oaks CA,
410 2019).

411 31. Wickham, H. *Ggplot2: Elegant Graphics for Data Analysis*. (Springer-Verlag, New York,
412 2016).
413 32. Love, M. I., Huber, W. & Anders, S. Moderated estimation of fold change and dispersion
414 for RNA-seq data with DESeq2. *Genome Biol* **15**, 550 (2014).
415 33. Hao, Y. *et al.* Integrated analysis of multimodal single-cell data. *Cell* **184**, 3573-3587.e29
416 (2021).
417

418 **Declarations**

419 *Ethics approval and consent to participate*

420 All research complied with relevant ethical regulations, and usage of human tissue material
421 and transcriptome data was approved by the ethics committee of the Medical Faculty at Kiel
422 University (A156/03, A124/14, A102/16).

423

424 *Consent for publication*

425 Not applicable

426

427 *Availability of data and material*

428 Not applicable. All data was retrieved (see method section).

429

430 *Competing interests*

431 SS reports indirect stock ownership in Gerion Biotech GmbH as well as consulting and
432 personal fees from AbbVie, Allergosan, Amgen, Arena, BMS, Biogen, Celltrion, Celgene, Falk,
433 Ferring, Fresenius, Galapagos/Gilead, HIKMA, I-Mab, Janssen, Lilly, Morphic, MSD, Mylan,
434 Pfizer, Prometheus, Protagonist, Provention Bio, Sandoz/Hexal, Takeda, and Theravance. PR
435 reports stock ownership in Gerion Biotech GmbH and consulting fees from Takeda.

436 All other authors declare no competing interests.

437

438 *Funding*

439 This work was supported by the German Research Foundation (DFG) through the individual
440 grant SO1141/10-1, the Research Unit FOR5042 “miTarget - The Microbiome as a Target in
441 Inflammatory Bowel Diseases” (project P5), the Excellence Cluster EXS2167 “Precision
442 Medicine in Chronic Inflammation” and an intramural grant of the medical faculty of Kiel
443 University (grant no K126408) to FS. The funding bodies had no part or influence on the design
444 of the study and data collection, analysis, or interpretation.

Authors' contributions

SW, LJ and FS designed research. SW, JT, LJ and FS performed experiments and analyzed the data. SS, CR, KA and PR provided samples and RNAseq data. SW, JT, LJ and FS prepared the figures. KA, PR, CK and FS obtained funding. SW, JT, LJ and FS co-wrote the manuscript with critical input from all authors. All authors read and approved the final manuscript.

Acknowledgements

The authors thank Sabine Kock, Stefanie Baumgarten, Maren Reffelmann, Vivian Wegner, Tanja Klostermeier, Dorina Ölsner, Meike Hansen, Ronja Möhring and Sophie Reiher for excellent technical assistance. We further thank Florian Tran and Finn Hinrichsen for valuable input regarding the description of the clinical cohort characteristics.

Authors' information (optional)

Not applicable

461 **Figures and tables**

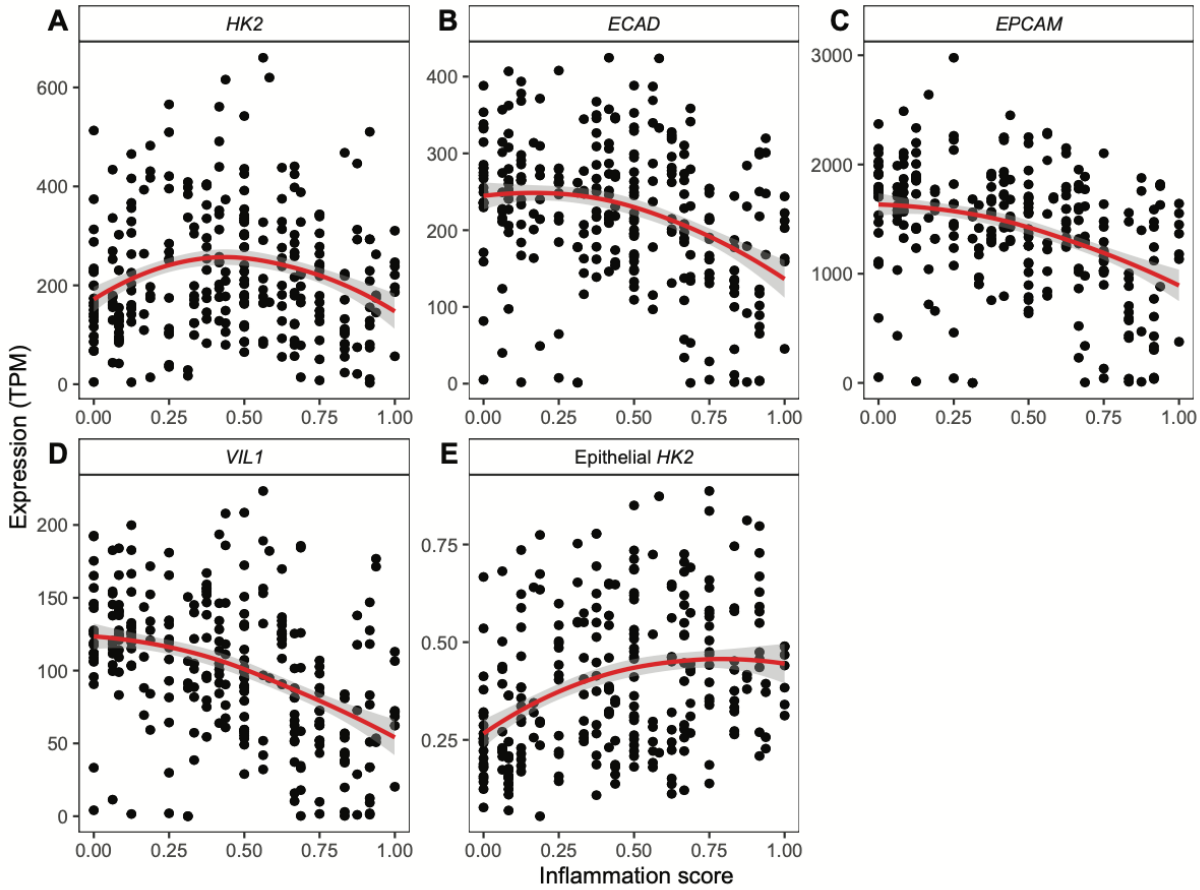

462

463 **Figure 1: Epithelial HK2 expression correlates with inflammation severity. A-D)** Expression
464 (TPM, transcript per million) of *HK2* **(A)** and the epithelial marker genes *ECAD* **(B)***, VIL1* **(C)** and
465 *EPCAM* **(D)** in the intestinal mucosa of patients with various degrees of gut inflammation.
466 Note that at high inflammation scores (>0.4) expression of *HK2* and the epithelial marker
467 genes all decrease indicating epithelial erosion. The inflammation score was calculated as a
468 scaled Harvey-Bradshaw index (Crohn's disease) or Mayo score (ulcerative colitis) to
469 accommodate both disease types. **E)** *HK2* expression increases with inflammation scores after
470 normalization to epithelial marker gene expression. The red lines represent the mean
471 expression trendline. The number in the upper right corner represents the p value for the
472 correlation between gene expression and inflammation score as determined by linear mixed
473 model.

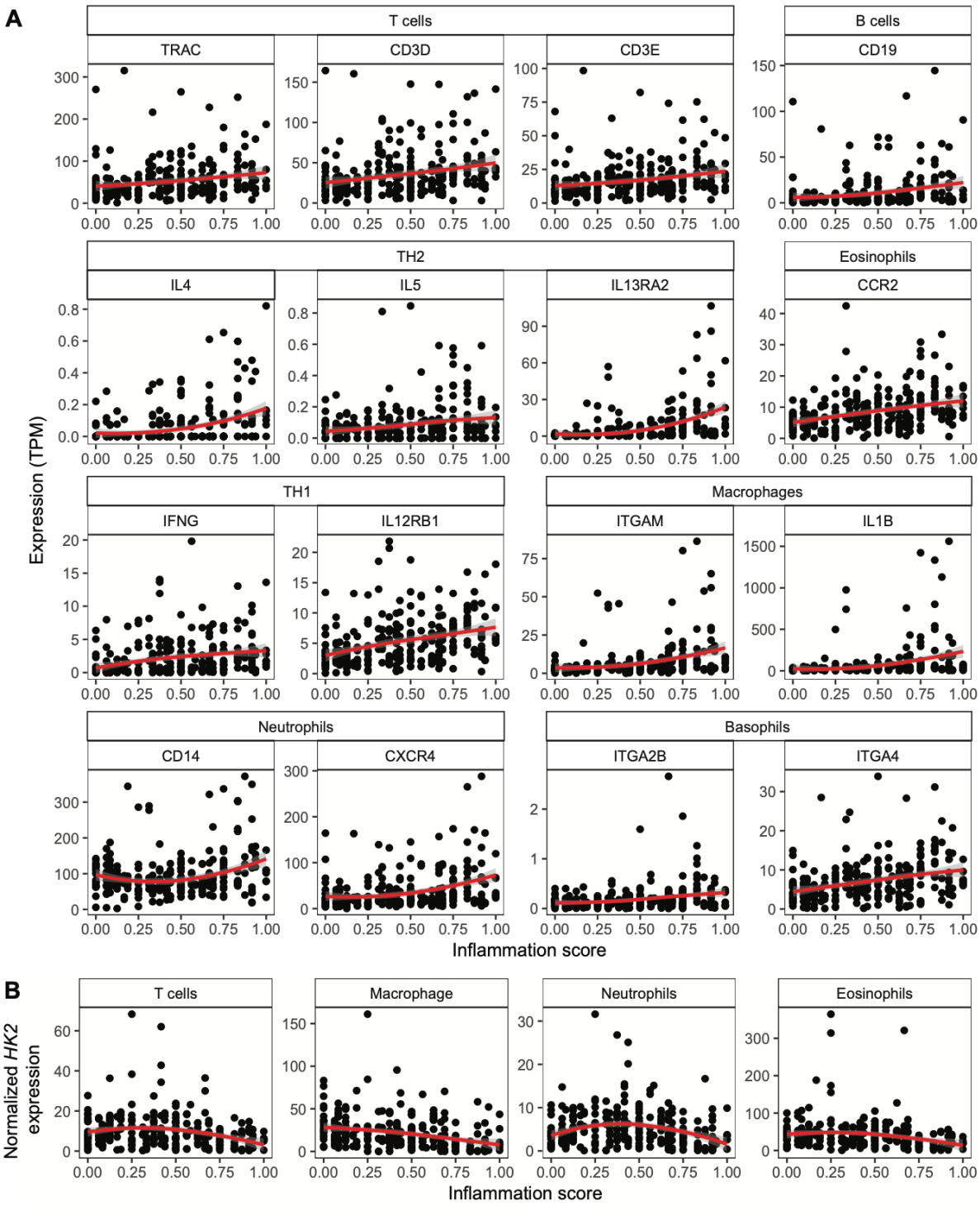

Figure 2: Expression of candidate immune marker genes increases with inflammation severity. Expression of selected marker genes, which are characteristic for individual immune cell types, were evaluated in patient biopsies. Expression of virtually all candidate immune marker genes increase with inflammation severity indicating an expansion of immune cells – a known feature of intestinal inflammation.

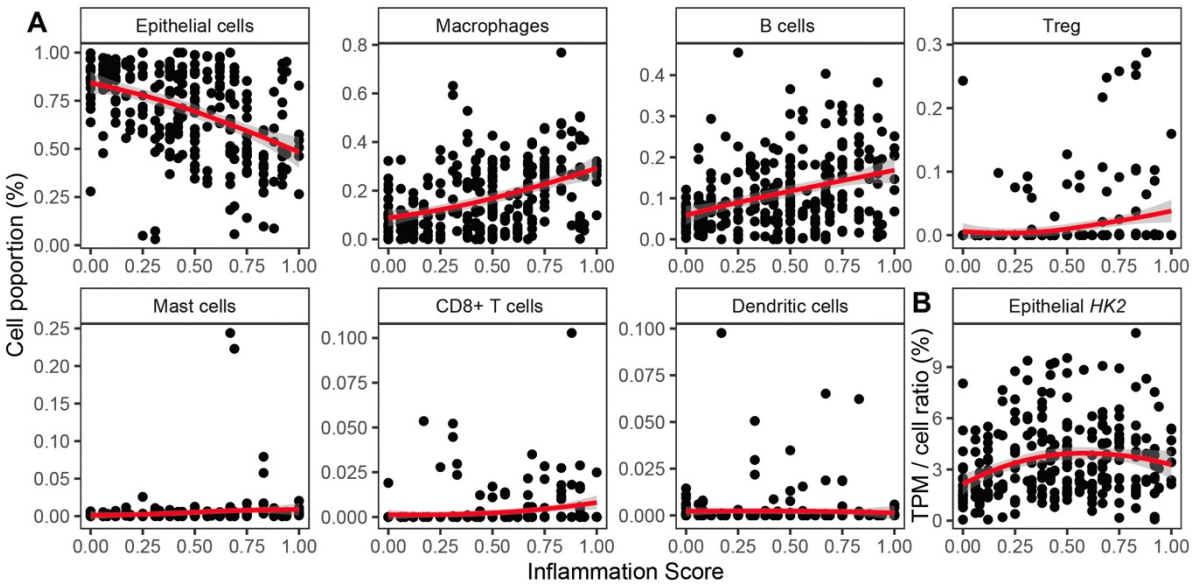

480

481 **Figure 3: Deconvolution of mucosal transcriptomes demonstrates cellular remodeling**
482 **during inflammation. A)** MuSiC cell deconvolution package was used to estimate ratios of the
483 most abundant cell types based on the mucosal patient transcriptomes. Notably, epithelial
484 cell abundance is decreasing with inflammation, whereas abundances of macrophages and B
485 cells, the two most frequent immune cell types that combine for approximately 35 %
486 proportion, are increasing with inflammation severity. Therefore, cell deconvolution supports
487 the candidate gene analyses indicating mucosal cellular remodeling characterized by a
488 reduction of epithelial cells and an expansion of immune cells with increasing inflammation
489 severity. **B)** *HK2* expression increases with inflammation scores after normalization to
490 epithelial cell abundance.

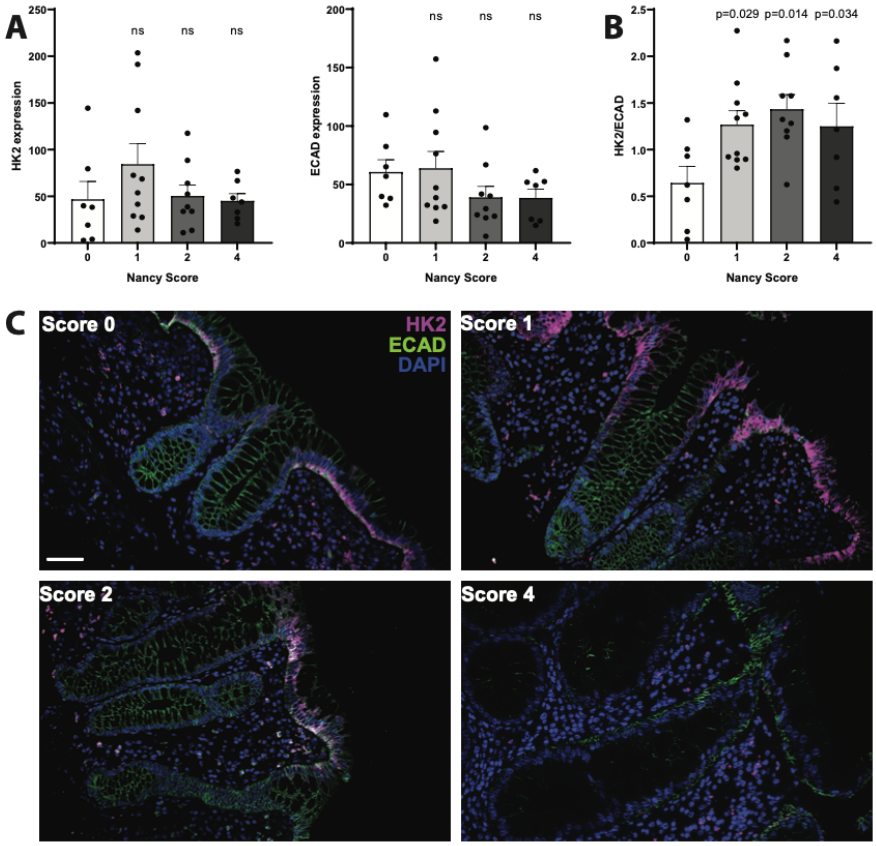

Figure 4: Epithelial HK2 protein expression increases with inflammation severity. Colonic mucosa biopsies of unrelated UC patients were stained for HK2, epithelial cells (ECAD) and nuclei (DAPI). All biopsies were analyzed for classical histological signs of inflammation using the Nancy Score (see method section). **A)** Quantification of HK2 and ECAD signal intensity in apical intestinal epithelium. Note that HK2 and ECAD level decrease with higher Nancy Scores. **B)** HK2 protein expression normalized to ECAD levels. Note that after epithelial normalization HK2 expression increases with inflammation severity, i.e. Nancy Score. Significance testing was performed using one-way ANOVA compared to Score = 0. **C)** Representative images of the multiplex immunofluorescence stainings (HK2, ECAD, DAPI). Scale bar indicates 50 µm. n = 7 – 10 per group. Note that microscopic images were taken from areas with rather intact epithelium for a better visualization of the mucosal structure.

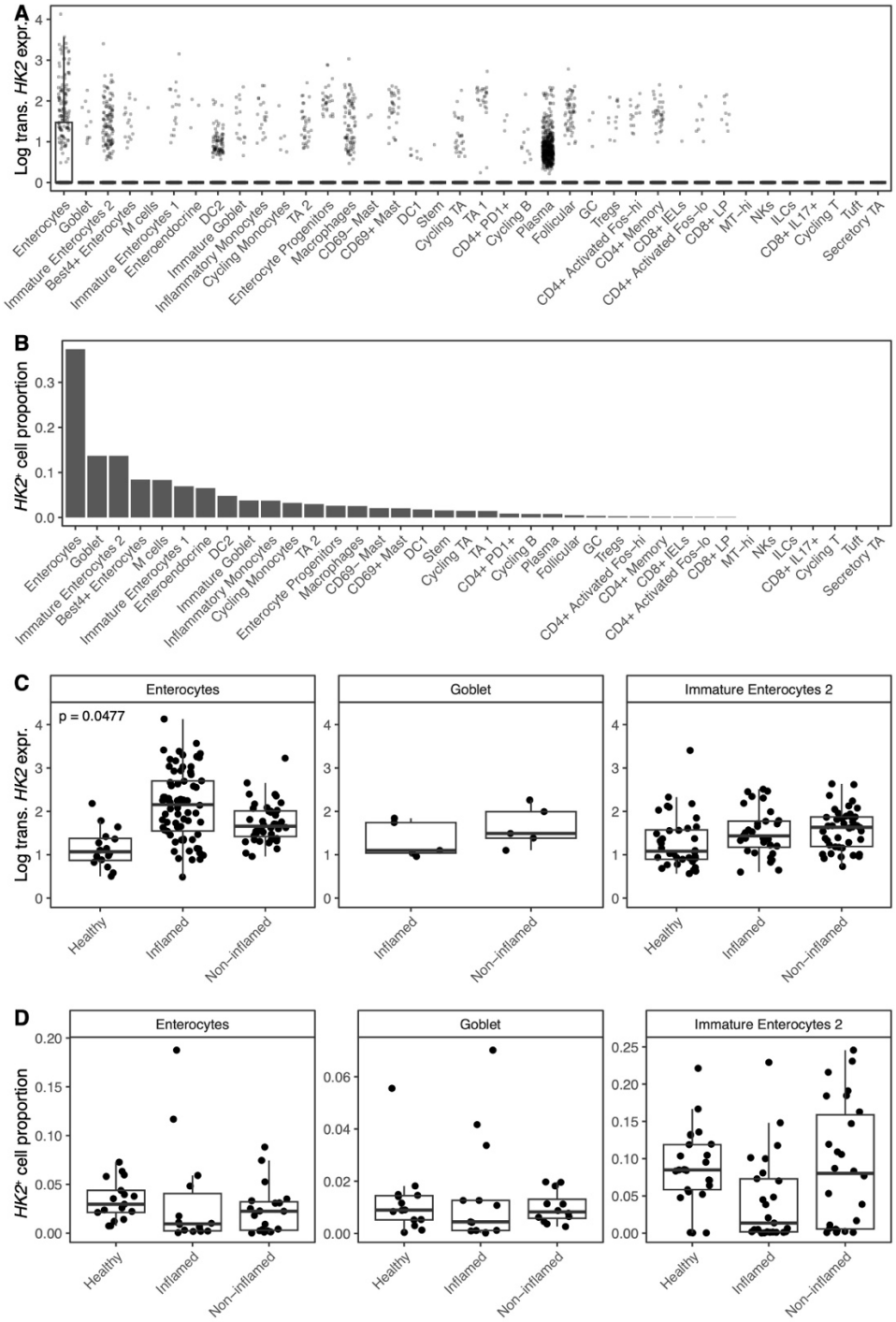

503

504 **Figure 5: *HK2* is mainly expressed by mature enterocytes and increased during**
505 **inflammation.** *HK2* expression was analyzed in published single cell RNA sequencing data
506 derived from mucosal biopsies of UC patients[11]. **A)** *HK2* expression per cell type. **B)**
507 Abundances of cell types expressing *HK2*. **C)** *HK2* expression in mature & immature
508 enterocytes and goblet cells divided into samples from healthy controls, inflamed and non-
509 inflamed mucosa. **D)** Abundances of cell types expressing *HK2* after stratification into disease
510 group.

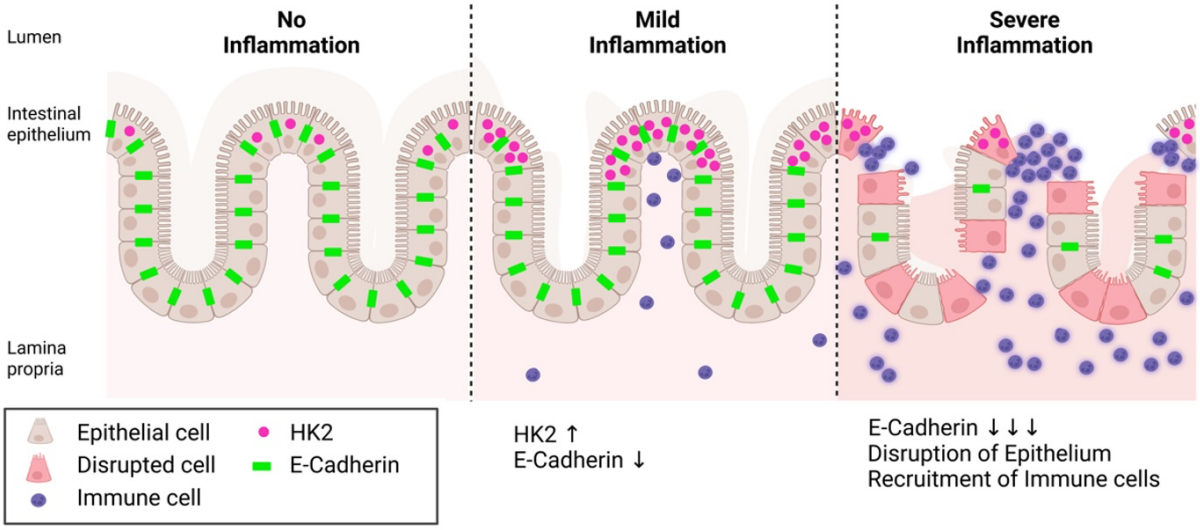

Figure 6: Model of HK2 expression changes in relation to intestinal inflammation severity. HK2 is predominantly expressed by apical epithelial cells and HK2 expression in these cells increases with disease severity. However, during the course of inflammation the cellular composition of the mucosa changes. In severely inflamed tissue, the epithelium is disrupted, brush border epithelial cells with high levels of HK2 are shed and lost, whereas immune cells with little to no HK2 expression are recruited. Therefore, overall HK2 expression is reduced in bulk tissue samples under severe inflammation despite local high expression in remaining HK2-positive epithelial cells. Created with BioRender.com

521 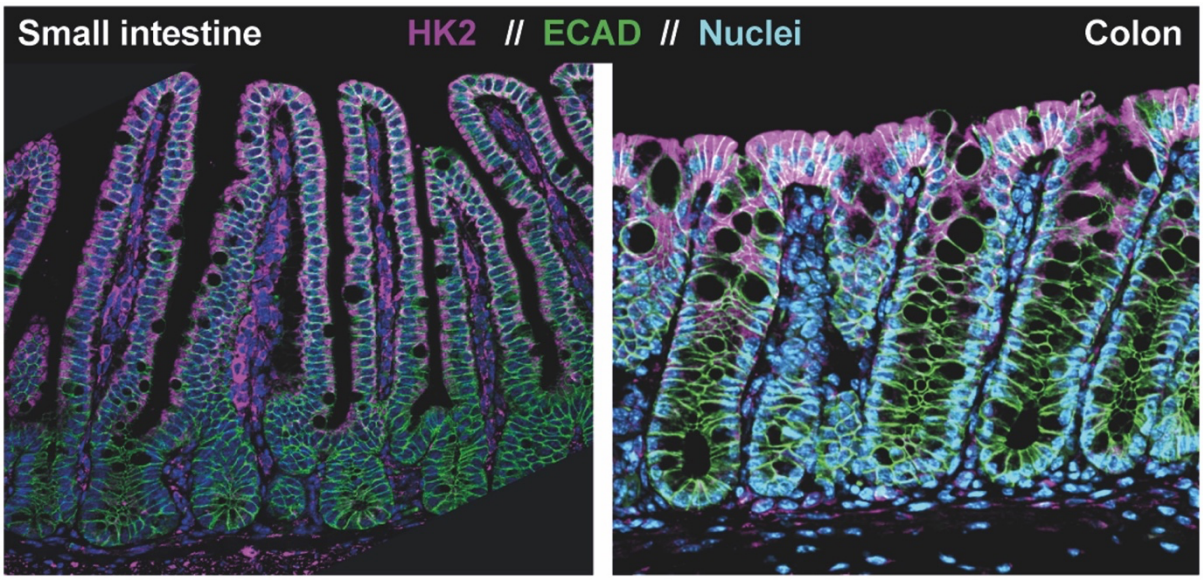

522 **Figure S1: HK2 expression in the intestinal mucosa.** Biopsies from small and large intestine
523 were immuno-stained to localize the HK2 protein in the mucosa. Note that HK2 expression is
524 mainly confined to epithelial cells of the apical mucosa both in the small and large intestine.

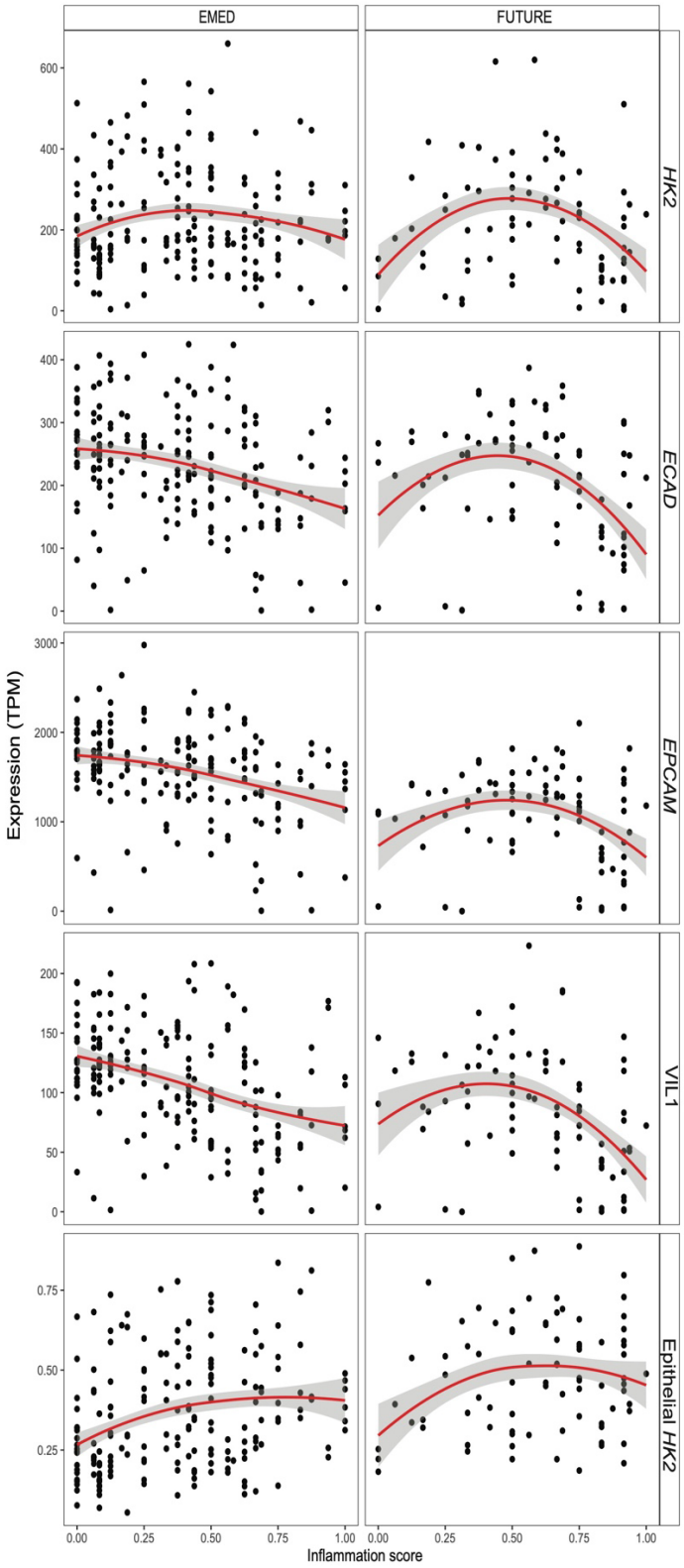

525

526 **Figure S2: Epithelial *HK2* expression correlates with disease severity in both clinical cohorts.**
527 Expression data (TPM, transcript per million) of *HK2* and the epithelial marker genes *ECAD,*
528 *VIL1* and *EPCAM* in the intestinal mucosa of patients with various degrees of gut inflammation
529 split per clinical cohort FUTURE and EMED.

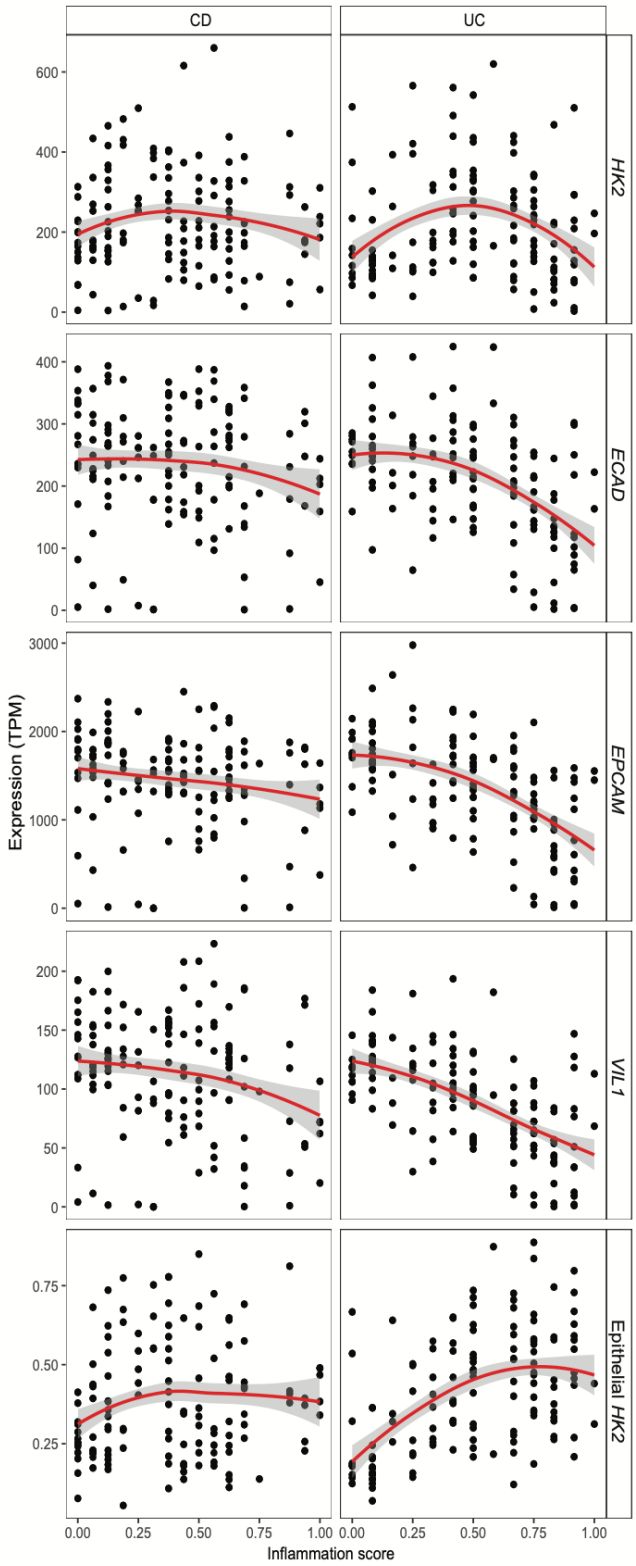

530

531 **Figure S3: Epithelial *HK2* expression correlates with inflammation severity regardless of**
532 **disease subtype.** Expression data (TPM, transcript per million) of *HK2* and the epithelial
533 marker genes *ECAD, VIL1* and *EPCAM* in the intestinal mucosa of patients with various degrees
534 of gut inflammation split per disease subtype CD and UC.

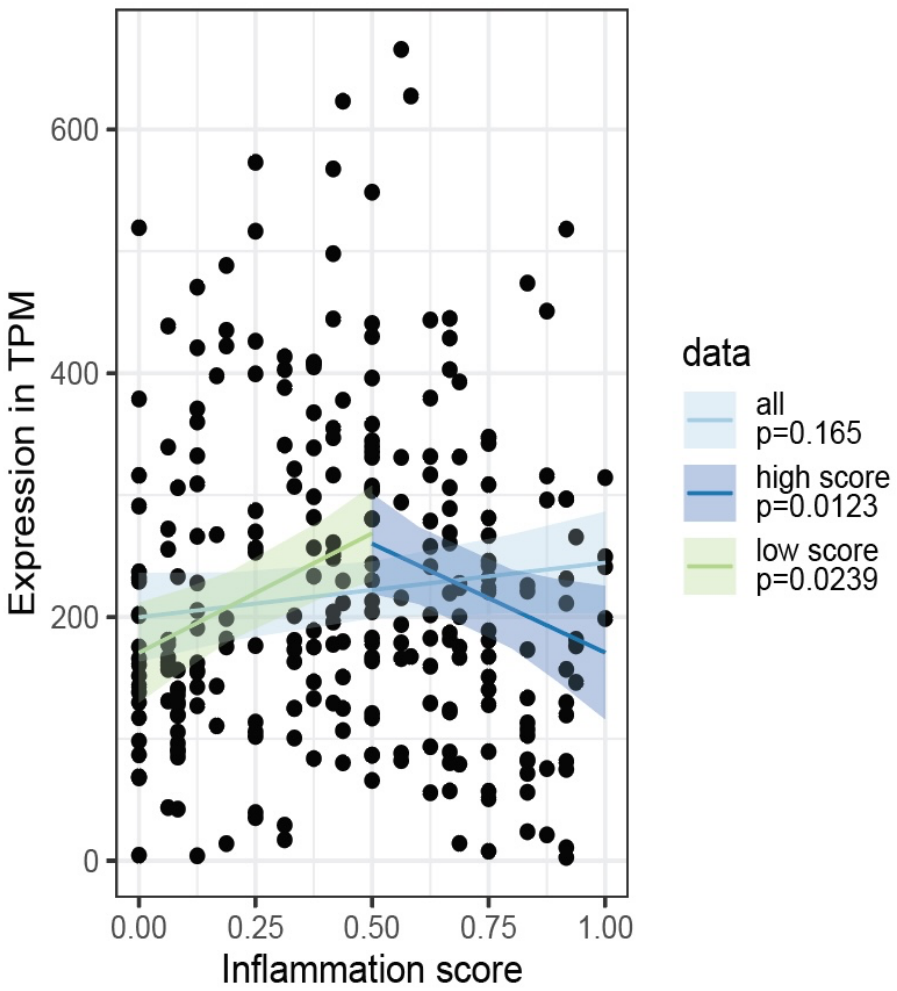

535

536 **Figure S4: Correlation analysis for HK2 expression and inflammation score.** Three different
537 linear mixed effect models (PatientID as random factor) were fitted to the data. First, all data
538 points were used to estimate the overall effect of *HK2* expression and inflammation score.
539 Afterwards the data set was split into “low scores” (inflammation score < 0.5), "high scores”
540 (inflammation score >0.5) and fitted models for these data subsets. While the first model
541 showed no significant association between *HK2* expression and inflammation, there is a
542 positive association at “low scores” and a negative association at “high scores” (see also table
543 S2) indicating that *HK2* expression increases with inflammation during lower disease scores
544 and then decreases at higher disease scores.

545 **Table S1: Cohort clinical characteristics**

Cohort	EMED	FUTURE	Combined	CD	UC
Patients	41	16	57	28	29
Samples	191	87	278	141	137
Age in years, min - max (median)	21 - 65 (26)	16 -74 (36)	16 - 74 (35)	16 - 74 (35)	18 - 65 (35)
Sex assigned at birth	57 female 30 male	119 female 72 male	176 female 102 male	95 female 56 male	81 female 56 male
Smoking	5 smoker 17 previous 65 non-smoker	53 smoker 30 previous 108 non-smoker	58 smoker 47 previous 173 non-smoker	40 smoker 25 previous 76 non-smoker	18 smoker 22 previous 97 non-smoker
Age at first diagnosis in years, min - max (median)	6 - 60 (22)	3 -61 (25)	3 - 61 (24)	3 - 61 (22)	13 - 60 (26)
Time since first diagnosis in years, min - max (median)	0 - 20 (4)	0 - 29 (9)	0 - 29 (6)	0 - 27 (8)	0 - 29 (5)
Inflammation score, min - max (median)	0 - 1 (0.375)	0 - 1 (0.625)	0 - 1 (0.4375)	0 - 1 (0.5)	0 - 1 (0.375)

546

547 **Table S2: Comparison of linear mixed model statistics for the coefficients explaining HK2**
548 **expression with inflammation scores for models created with all data, low (score <0.5) or**
549 **high (score >0.05) inflammation scores only.**

	Estimate	Std. Error	DF	t-value	p-value	
All data	44.73	32.07	179.94	1.395	0.165	
Low score	195.86	59.48	154.44	3.293	0.0123	**
High score	-178.6	78	114.87	-2.29	0.0239	*

550

551 **Table S3: Translation of the HBI and Mayo Score into a general Inflammation Score.** The
552 definitions of the HBI and Mayo scores are listed. The Inflammation Score was calculated by
553 scaling each the HBI and Mayo Score from 0-1 and then merging the scores.

HBI		
Criterium	**Score**	
General well-being	Very well	0
	Slightly poor	1
	Poor	2
	Very poor	3
	Terrible	4
Abdominal pain	None	0
	Mild	1
	Moderate	2
	Severe	3
Abdominal mass	None	0
	Dubious	1
	Definite	2
	Definite with tenderness	3
Stool frequency	Number of liquid stools	1 for each lquid stool per day
Complications	Arthralgia, Uveitis, Erythema nodosum, Apthous ulcers, Pyoderma gangrenosum, Anal fissure, New fistula, Abscess	1 point each

554

Mayo Score		
Criterium	**Score**	
Number of stools per day	Normal for the patient	0
	1-2 stools more than normal	1
	3-4 stools more than normal	2
	5+ stools more than normal	3
Rectal blood	No blood	0
	Blood streaks in less the half of evacuations	1
	Evidence of fresh blood in most of the evacuations	2
	Bowel movements with fresh blood	3
Endoscopy	Normal or inactive disease	0
	Mild disease (erythema, decreased vascular pattern, mild friability)	1
	Moderate disease (marked erythema, lack of vascular pattern, friability, erosions)	2
	Severe disease (spontaneous bleeding, ulceration)	3
Global medical asessment	Normal	0
	Mild disease	1
	Moderate disease	2
	Severe disease	3

555
556

Calculation of inflammation score										
HBI	**InfScore**		**Mayo**	**InfScore**		**>>>**		**InfScore**	**HBI**	**Mayo**
0	0.00		0	0.00		merged		0.00	0	0
1	0.06		1	0.08				0.06	1	
2	0.12		2	0.17				0.08		1
3	0.18		3	0.25				0.12	2	
4	0.24		4	0.33				0.17		2
5	0.29		5	0.42				0.18	3	
6	0.35		6	0.50				0.24	4	
7	0.41		7	0.58				0.25		3
8	0.47		8	0.67				0.29	5	
9	0.53		9	0.75				0.33		4
10	0.59		10	0.83				0.35	6	
11	0.65		11	0.92				0.41	7	
12	0.71		12	1.00				0.42		5
13	0.76							0.47	8	
14	0.82							0.50		6
15	0.88							0.53	9	
16	0.94							0.58		7
17	1.00							0.59	10	
								0.65	11	
								0.67		8
								0.71	12	
								0.75		9
								0.76	13	
								0.82	14	
								0.83		10
								0.88	15	
								0.92		11
								0.94	16	
								1.00	17	12

559 **Table S4: Original and pooled deconvolution cell types.** Originally classified cell types that
560 are ontogenetically related, e.g. Paneth cells, enterocytes, goblet cells and stem cells, were
561 pooled and classified into "epithelial cells" to reduce cell type diversity.

Original cell type description	Grouped into cell type
TA 1	epis
TA 2	epis
Enterocyte Progenitors	epis
Immature Goblet	epis
Immature Enterocytes 1	epis
Immature Enterocytes 2	epis
Cycling TA	epis

562